Cytotherapy, 2014; 16: 1059–1072

International Society for Cellular Therapy
ISCT®

Human mesenchymal stromal cell transplantation modulates neuroinflammatory milieu in a mouse model of amyotrophic lateral sclerosis

MARINA BOIDO[1], ANTONIO PIRAS[1,*], VALERIA VALSECCHI[1,*], GIADA SPIGOLON[1], KATIA MARESCHI[2], IVANA FERRERO[2], ANDREA VIZZINI[1], SANTA TEMI[1], LETIZIA MAZZINI[3], FRANCA FAGIOLI[2] & ALESSANDRO VERCELLI[1]

[1]*Neuroscience Institute Cavalieri Ottolenghi, Department of Neuroscience, University of Torino, Torino, Italy,* [2]*Paediatric Onco-Haematology, Stem Cell Transplantation and Cellular Therapy Division, City of Science and Health of Turin, Regina Margherita Children's Hospital, Department of Public Health and Paediatrics, University of Torino, Torino, Italy, and* [3]*ALS Centre Department of Neurology, University of Eastern Piedmont, Novara, Italy*

Abstract

Background aims. Mesenchymal stromal cells (MSCs), after intraparenchymal, intrathecal and endovenous administration, have been previously tested for cell therapy in amyotrophic lateral sclerosis in the SOD1 (superoxide dismutase 1) mouse. However, every administration route has specific pros and cons. *Methods.* We administrated human MSCs (hMSCs) in the cisterna lumbaris, which is easily accessible and could be used in outpatient surgery, in the SOD1 G93A mouse, at the earliest onset of symptoms. Control animals received saline injections. Motor behavior was checked starting from 2 months of age until the mice were killed. Animals were killed 2 weeks after transplantation; lumbar motoneurons were stereologically counted, astrocytes and microglia were analyzed and quantified after immunohistochemistry and cytokine expression was assayed by means of real-time polymerase chain reaction. *Results.* We provide evidence that this route of administration can exert strongly positive effects. Motoneuron death and motor decay were delayed, astrogliosis was reduced and microglial activation was modulated. In addition, hMSC transplantation prevented the downregulation of the anti-inflammatory interleukin-10, as well as that of vascular endothelial growth factor observed in saline-treated transgenic mice compared with wild type, and resulted in a dramatic increase in the expression of the anti-inflammatory interleukin-13. *Conclusions.* Our results suggest that hMSCs, when intracisternally administered, can exert their paracrine potential, influencing the inflammatory response of the host.

Key Words: *cell therapy, cisterna lumbaris, cytokines, microglia, motoneuron*

Introduction

Amyotrophic lateral sclerosis (ALS) is a late-onset neurodegenerative disease that causes degeneration and death of upper and lower motoneurons, leading to weakness, muscle atrophy, fasciculations, spasticity and finally, death as the result of respiratory failure (1). Currently, there is no treatment for ALS. Riluzole, the only drug approved by the Food and Drug Administration for ALS, has a very limited outcome because it increases survival by only 2–3 months compared with placebo (2).

In the past decade, stem cell therapy emerged as a possible strategy to modulate the motoneuron environment, in terms of astrogliosis and microglial activation that occur in ALS, and to deliver trophic factors to support motoneuron survival (3,4). To this aim, several studies reported beneficial effects after transplantation of different types of stem cells in animal models of ALS: mesenchymal stromal cells (MSCs) (5–7), neural stem cells (8–11), olfactory ensheathing cells (12) and induced pluripotent cells (13); also, clinical trials have demonstrated the feasibility of human MSC (hMSC) transplantation in patients (14–16). The cell type that better matches safety conditions and immunomodulatory/neurotrophic roles consists of MSCs. MSCs are bone marrow (BM) cells expanded *ex vivo* (17); they represent a small fraction (0.001–0.01%) of the BM

*These authors contributed equally to this work.
Correspondence: **Marina Boido**, MSc, PhD, Neuroscience Institute Cavalieri Ottolenghi, Department of Neuroscience, Regione Gonzole 10, 10043 Orbassano (TO), Italy. E-mail: marina.boido@unito.it

(Received 22 October 2013; accepted 9 February 2014)

http://dx.doi.org/10.1016/j.jcyt.2014.02.003

cell population. Although BM is the best characterized source of MSCs, umbilical cord blood, Wharton's jelly, placenta, adipose tissue and many others represent promising alternatives (18). Several groups, including ours (6), have shown that MSC transplantation can delay the behavioral symptoms and motoneuron death in animal models of ALS (4). MSCs have been delivered intraparenchymally, intrathecally, intramuscularly or intravenously, each of which has its own advantages and disadvantages (4). In the present study, we decided to administer MSCs in the cisterna lumbaris, which is easily accessible and could be used in outpatient surgery, in an animal model of ALS, the SOD1 (superoxide dismutase 1) G93A mouse, at the earliest onset of symptoms. We provide evidence that this route of administration can exert positive effects. Additionally, we analyzed the expression of several pro-inflammatory and anti-inflammatory cytokines by the host, identifying one of the hMSC mechanisms of action.

Methods

Animal care and use

Experiments were performed on male transgenic mice B6SJL-TgN(SOD1G93A)1Gur over-expressing human SOD1, containing the Gly93 to Ala mutation (Jackson Laboratory, Bar Harbor, ME, USA; stock No. 002726); these mice have a high transgene copy number, as reported in the data sheet. Founders were kindly gifted by M. Bentivoglio and R. Mariotti (University of Verona). The colony was derived by breeding of male transgenic mice to naive (B6xSJL/J)F1 female mice (Janvier SAS, Le Genest-Saint-Isle, France).

All experimental procedures on live animals were carried out in strict accordance with the European Communities Council Directive 86/609/EEC (November 24, 1986) Italian Ministry of Health and University of Turin institutional guidelines on animal welfare (law 116/92 on Care and Protection of living animals undergoing experimental or other scientific procedures; authorization No. 17/2010-B, June 30, 2010); additionally, an ad hoc Ethical Committee of the University of Turin approved this study. All efforts were made to minimize the number of animals used and their suffering. They were identified by polymerase chain reaction (PCR) according to Jackson Laboratory's genotyping protocol.

Genotyping mice

DNA from mouse tail was extracted by incubation of a 0.5-cm-long specimen of tail in 100 µL of lysis buffer (10 mmol/L Tris HCl, 50 mmol/L KCl, 0.01% gelatin, 0.45% IGEPAL® CA-630 [Sigma-Aldrich], 0.4% Tween-20) and 25 µg of proteinase K at 55°C overnight under gentle shaking. On the extracted DNA, we performed PCR to evaluate the presence of the human transgene superoxide dismutase-1 (hSOD1). The primers used, suggested by Jackson Laboratories, were 5′-CATCAGCCCTAATCCATCTGA-3′ and 5′-CGCGACTAACAATCAAAGTGA-3′ for *hSOD1* gene and 5′-CTAGGCCACAGAATTGAAAGATCT-3′ and 5′-GTAGGTGGAAATTCTAGCATCATCC-3′ for mouse interleukin 2 gene (*mIL-2*), as internal control.

Behavioral tests

To treat the animals at the symptom onset, the mice (hMSC TG, $n = 16$; sal TG, $n = 14$) were weighed weekly and underwent a battery of behavioral tests starting from the asymptomatic phase: scoring of motor deficits by a trained observer (6), rotarod and paw grip endurance (PaGE) tests (19).

The first 2 weeks of tests (starting around postnatal day 60 [P60]) were considered as training for the animals that were tested weekly. Thereafter, the tests were performed twice per week.

The values obtained before onset of symptoms were considered as baseline to be compared with those obtained after treatment until the mice were killed at 14 days after grafting, to evaluate the effects of hMSCs on the decay in behavioral performance caused by disease.

The neurological test was performed in an open field [size: 70 (width) × 120 (depth) cm] to assess gait; the mice were evaluated for signs of motor deficits with the following -point scoring system: 4 points if normal (no sign of motor dysfunction); 3 points if hind limb tremors were evident when suspended by the tail; 2 points if gait abnormalities were present; 1 point for dragging of at least one hind limb; 0 points for inability to right itself within 30 seconds.

For the rotarod test, we measured the time animals could remain on the rotating cylinder in a 7650 accelerating model of a rotarod apparatus (Ugo Basile, Comerio, Va, Italy). Each animal was given three trials. The arbitrary cut-off time was 300 seconds, and the accelerated speed went from 4 to 32 rpm. The size of rotarod equipment is 40 (width) × 30 (depth) × 38 (height) cm, and the rotating cylinder diameter is 3 cm.

For the PaGE test, the animal was placed on the wire lid of conventional housing cage [size: 38 (width) × 22 (depth) cm]. The lid was gently shaken to prompt the mouse to hold onto the grid before it was swiftly turned upside down. Grip score was

measured as the length of time that the mouse was able to hang on to the grid. The arbitrary cut-off time was 90 seconds.

Isolation and characterization of hMSCs

BM cells were harvested from the iliac crest of adult or pediatric donors who underwent BM collection for a related patient after written informed consent, in accordance with the ethics committee of the hospitals Ospedale Infantile Regina Margherita-Sant'Anna-Mauritian order, which approved the collection of BM cells.

The cells were counted and plated directly in MSC Growth Medium (MesenCult Proliferation Kit, Stemcell Technologies, Vancouver, Canada) containing 10% fetal bovine serum at the density of 100,000 cells/cm^2 in T25 or T75 flasks (Becton Dickinson, Franklin Lakes, NJ, USA) and maintained at 37°C with an atmosphere of 5% CO_2. After 5 days, the non-adherent cells were removed and re-fed every 3 to 4 days. At confluence, cells were detached or re-plated at 10^3 cells/cm^2 for 3 to 5 more passages. The cells were counted and analyzed at each passage for cellular growth, viability, immunophenotype and multipotent capacity, as described previously (20–22).

Twenty-four hours before transplantation, 10 μg/mL of bisbenzimide (Sigma, St Louis, MO, USA) was added to the culture medium to label the cell nuclei. The cells were then resuspended in saline solution to obtain a final concentration of 60,000 cells/μL to be used for transplantation.

hMSC transplantation

Mice were divided into three groups: (i) SOD1 transgenic mice (hMSC TG; $n = 16$), which had 300,000 hMSCs, in a volume of 5 μL of saline solution, injected into the cisterna lumbaris; (ii) SOD1 untreated mice (sal TG; $n = 14$), which received 5 μL of saline solution injected into the cisterna lumbaris and (iii) wild-type mice (sal WT, $n = 10$), 5 μL of saline solution injected into the cisterna lumbaris. The amount of hMSCs used for transplantation was based on previous studies indicating that injections of 300,000 cells (23) were more effective than 100,000 intrathecal cells (24).

When TG mice showed decay in performance twice (i.e., when the animals displayed decreased motor behavior in two consecutive testing sessions), they underwent surgery and were killed 2 weeks later. Age-matched WT mice were killed. Briefly, mice were deeply anaesthetized with 3% isoflurane vaporized in O_2/N_2O 50:50. The lumbar spine was exposed, and spinal muscles were displaced laterally; the injections were performed at the L5-L6 intervertebral space (25) with the use of a glass micropipette (outer tip diameter, 50 μm) connected to a syringe body by a silicon tube. hMSCs/saline was slowly injected (over approximately 60 seconds) into the cisterna lumbaris. The wound was then sutured, and the mice were returned to their cages.

Histological examination

Two weeks after transplantation, a group of animals (hMSC TG, $n = 9$; sal TG, $n = 8$; WT, $n = 5$) were deeply anesthetized as previously described and underwent intracardiac perfusion with 4% buffered paraformaldehyde, pH 7.4. The lumbar spinal cords were removed and post-fixed in paraformaldehyde for 2 h at 4°C. Additionally we randomly checked the hMSC presence at thoracic and cervical levels.

Samples were transferred overnight into 30% sucrose in 0.1 mol/L phosphate buffer at 4°C for cryoprotection, embedded in cryostat medium (Killik; Bio-Optica, Milan, Italy) and cut on the cryostat (Microm HM 550) in serial transverse 50-μm-thick sections, kept in phosphate-buffered saline (PBS) at 4°C or mounted onto gelatin-coated slides, to be processed for immunostaining.

Before any further reaction, all sections were mounted in PBS, coverslipped and examined with the use of a Nikon Eclipse E800 epifluorescence microscope under 4′-6-diamidino-2-phenylindole (DAPI) filter set to check the transplanted hMSC survival.

Immunofluorescence

For immunofluorescence, after unspecific binding sites were blocked for 30 min at room temperature with 0.3% Triton X-100 and 10% normal donkey serum (Sigma-Aldrich) in PBS, pH 7.4, the sections were incubated with the following primary antibodies at 4°C overnight [for the origin and specificity of the antibodies see also Uccelli *et al.* (5)]: polyclonal anti-glial fibrillary acidic protein (GFAP) (rabbit; 1:500; DakoCytomation, Glostrup, Denmark), polyclonal anti-ionized calcium binding adaptor molecule 1 (IBA1) (rabbit, 1:1000; Wako Chemicals, Neuss, Germany), monoclonal anti-neuronal nuclei (mouse; 1:10; Chemicon, Temecula, CA, USA) and monoclonal anti-human nuclei (mouse; 1:100, Millipore, Temecula, CA, USA).

The sections were then washed in PBS and incubated in 1:200 cyanine 3–conjugated secondary antibodies anti-rabbit or anti-mouse (1:200; Jackson ImmunoResearch Laboratories; West Grove, PA, USA).

The sections were examined with the use of a Nikon Eclipse 90i epifluorescence microscope and

photographed with the use of a Nikon DS-5Mc digital camera. Photomicrographs (except for those used for GFAP and IBA1 quantification) were manipulated and mounted in plates with the Photoshop CS2 software, with the use of autocontrast enhancement. To make three-dimensional reconstructions, some preparations were also examined with the use of a Leica TCS SP5 confocal laser scanning microscope.

To evaluate glial involvement, GFAP immunoreactivity in 12 spinal cords (6 hMSC TG versus 6 sal TG) and IBA1 immunoreactivity in 6 spinal cords (3 hMSC TG versus 3 sal TG) were analyzed. For semi-quantitative analysis, we considered L5 spinal cord level. In particular, we quantified GFAP immunoreactivity in ventral horns (laminae VIII-IX). These areas were identified with the use of a Nikon Eclipse 90i epifluorescence microscope and photographed with the use of the Nikon DS-5Mc digital camera (at 40×). The percentage of the overall GFAP-positive area was quantified with the use of Scion Image software for Windows (freeware version of NIH image, Scion Corporation, Frederick, MD, USA) by an observer who was blinded to the group identity of the specimens examined. We classified IBA1−positive microglial cells as "ramified" and "amoeboid"; we obtained a mean number of cell profiles/animal in sal TG and hMSC TG groups.

Nissl staining

One series of serial lumbar sections (one every 400 μm) from each animal was Nissl-stained to perform stereological counts. Sections were mounted on 2% gelatin-coated Superfrost slides and air-dried overnight; slides were hydrated in distilled water for 1 min before staining in 0.1% Cresyl violet acetate for 10 min, dehydrated in an ascending series of ethanol, cleared in xylene and cover-slipped with Eukitt (Bioptica, Milan, Italy).

Stereological counts

Motoneuron quantification was performed in sal WT ($n = 5$), sal TG ($n = 6$) and hMSC TG mice ($n = 6$). Their nucleoli were counted at 40× in the lumbar tract. Only neurons with an area $\geq$200 μm^2 (classified as alpha motoneurons) and located in a congruent position were counted (6,26).

A total estimated number of alpha motoneurons was obtained through the use of a stereological technique, the Optical Fractionator (27), by use of a computer-assisted microscope and the Stereo-Investigator software (MicroBrightField, Williston, VT, USA). Cells were counted on the computer screen with the use of an Optronics MicroFire digital camera mounted on a Nikon Eclipse E600 microscope.

We also calculated the total volume of the reconstructed segment (expressed in mm^3) and the motoneuron density expressed as number of motoneurons/mm^3.

Cytokine assays

Sal WT ($n = 5$), sal TG ($n = 6$) and hMSC TG mice ($n = 7$) were killed by means of cervical dislocation, and their lumbar spinal cord was rapidly dissected on ice. Total RNA from the spinal cord was extracted with the use of Trizol, following the supplier's instructions (Invitrogen, Milan, Italy). The first-strand complementary DNA (cDNA) was synthesized with 2 μg of total RNA with the use of the High Capacity cDNA Reverse Transcription Kit, following the supplier's instructions (Applied Biosystems, Monza, Italy).

The cDNAs from animals of each group were pooled together. This 50-ng sample of the mixed cDNAs was amplified by means of TaqMan reagent-based chemistry on TaqMan Array Plates (Applied Biosystems) containing 92 assays to detect mouse genes belonging to the immune response.

For single gene analysis, the cDNA of individual mice was analyzed for IL-10, IL-12a and IL-13 and vascular endothelial growth factor (VEGF) expression. The cDNA of each animal was previously pre-amplified with the use of the PreAmp Kit, following supplier's instructions (Applied Biosystems), and was then amplified with the use of the same TaqMan assay contained in the TaqMan Array Plate. All TaqMan gene expression assays have a PCR efficiency of 100% within measurement error (±10%). The amplifications were run in triplicate in one assay run. Beta-glucuronidase messenger RNA (mRNA) was used as housekeeping gene for data normalization. Changes in mRNA levels were determined as the difference in threshold cycle between target and housekeeping mRNA (ΔCt) followed by the comparative Ct method for relative quantification (ΔΔCt). All the reactions were performed on the StepOne Detection System (Applied Biosystems).

Statistical analysis

The data are expressed as mean ± standard error of the mean (SEM). For stereological counts and gene expression analysis, statistically significant differences among means were determined by one-way analysis of variance (ANOVA), followed by *post hoc* Newman-Keuls test. For astrogliosis and microglia activation, we used the unpaired *t*-test. For behavioral test analysis, inter-group differences were

statistically compared by means of two-way ANOVA. The thresholds for statistical significance data were set at $P < 0.05$. Statistical analysis was performed with the use of GraphPad Prism 5 software (GraphPad Software, San Diego, CA, USA).

Results

Engraftment of hMSCs

The hMSCs used in this study displayed the specific features defined by the International Society for Cellular Therapy guidelines, as previously demonstrated (22,28).

We injected 300,000 hMSCs into the cisterna lumbaris of early symptomatic SOD1 mice. After 2 weeks, we killed the animals and analyzed the spinal cords (Figure 1).

Grafted hMSCs were identified after pre-labeling with bisbenzimide. DNA-binding dyes such as bisbenzimide or DAPI could diffuse to the host tissue from dying labeled hMSCs, as suggested by other authors (29). However, they are used ordinarily as stem cell markers in grafts, in the absence of reports of dye diffusion (30–32). Moreover, we rarely observed dead hMSCs in this study and in the previous ones; also, we never found motoneurons, astrocytes or microglia labeled by bisbenzimide diffused from hMSCs. Additionally, to exclude the bisbenzimide leakage, we performed an immunofluorescence reaction against human nuclei antigen for specifically labeling hMSCs; as shown in

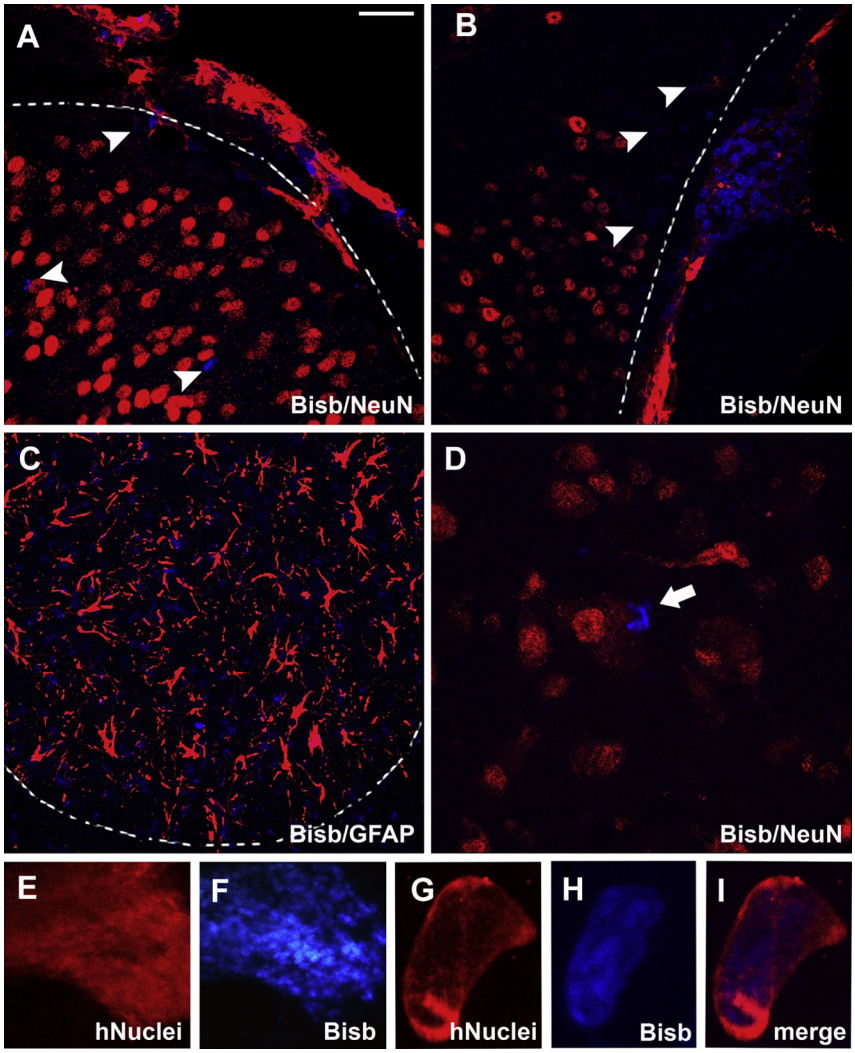

Figure 1. Human MSC engraftment. Two weeks after graft, bisbenzimide-positive hMSCs were observed in the lumbar tract. (A,B) hMSCs on the dorsal meninges (broken line identifies the spinal cord boundary), often penetrating into the spinal parenchyma (arrowheads). (C) hMSCs in the parenchyma of the ventral horn, outlined by broken line, (D) hMSCs in proximity of motoneurons. (E–I) Bisbenzimide-positive hMSCs also express human nuclei antigen, as shown at low (E and F, same magnification of C) and high (G–I) magnification. Scale bar = 30 μm in A, 32 μm in B, 50 μm in C, E and F, 20 μm in D and 3.5 μm in G–I.

Figure 1E–I, bisbenzimide-labeled MSCs are also human nuclei–positive.

We detected the highest number of hMSCs on the meninges, both ventrally and dorsally; however, we also detected a significant number of cells in the spinal parenchyma, even in the ventral horns in proximity of the motoneurons. hMSCs migrated cranially at a distance from the injection site. We observed cells mostly at the lumbar segment level and in reduced amounts at the lower thoracic level (T11-T12 vertebral segment). In one case, we observed surviving cells along the meninges up to the cervical level.

Stereological counts of lumbar motoneurons

Stereological counts showed significant inter-group differences in the motoneuron number (Table I): the number of motoneurons was greatly decreased in sal TG compared with sal WT ($P < 0.01$), but transplantation partially prevented motoneuron death because their number was significantly higher in hMSC TG than in sal TG ($P < 0.05$). Similar results were obtained regarding the total volume of anterior horn of the L1-L5 segment of the spinal cord and relative motoneuron density (Table I).

Behavioral tests

The decrease in motor performance in treated versus untreated SOD1 mice was evaluated with a battery of behavioral tests (neurological tests, rotarod test, PaGE test; Figure 2) as well as body weight measurements.

The first values reported in the graph (Figure 2) represent the scores obtained before the symptom appearance ("−39 days" in the graph); when mice showed two repeated deficits for two consecutive times, they were considered symptomatic and underwent surgery and hMSC/saline transplantation. The values in the graph at the "graft" time correspond to the last performance before transplantation. Mice were then killed 2 weeks later. Results concerning the body weight are shown differently, as described below.

The neurological test is described in Figure 2A. In this test, the first symptoms appeared later than with the following two tests; therefore, we considered it less reliable. In the sal TG mice, the deficits occurred earlier than in the hMSC TG, even though 14 days after graft, the final scores in the two groups were similar (2.9 ± 0.5 in treated mice versus 2.4 ± 0.5 in untreated mice); moreover, the change in score after surgery/transplantation was −1.36 ± 0.46 and −1.07 ± 0.48 in sal and hMSC TG mice, respectively.

The PaGE test is described in Figure 2B. This test evaluates the hind limb resistance. After the injection, the decline in performance is steady in both groups but slightly faster in the untreated animals (the last performance at "+14 days" was 21 ± 10 seconds for transplanted mice, 6 ± 2 seconds for sham-operated mice; $P < 0.01$). The decline observed from the graft day until the mice were killed was −41 ± 8 seconds in the treated animals versus −50 ± 5 seconds in the untreated animals.

The rotarod test is described in Figure 2C. This test measures motor performance and coordination of rodents. The performance just before the "graft" was statistically indistinguishable in the two transgenic groups; however, in the following days, the disease progression appeared earlier in the sal TG mice than in the hMSC TG mice, obtaining at 14 days the final values of 69 ± 23 seconds versus 134 ± 47 seconds in the untreated versus treated mice, respectively ($P < 0.05$). We observed a decrease in the time of performance (expressed in seconds) equal to −161 ± 30 for the untreated mice and −93 ± 53 for the treated mice.

We observed differences in body weight between the pre-symptomatic phase (17 days before graft) and the day the mice were killed (14 days after graft) in the SOD1 mice. The reduction of body weight in this period was 1.23 ± 0.64 g in the hMSC TG mice and 2.50 ± 0.96 g in the sal TG mice (difference not significant).

Reactive astrogliosis and microglial activation

Because neuroinflammation is strongly involved in ALS progression, we evaluated semiquantitatively the astroglial reaction in the ventral spinal horn by means of GFAP and IBA1 immuno-analysis

Table I. Stereological analysis of the lumbar spinal cord.

	sal WT	hMSC TG	sal TG
Motoneuron number	1947.34 ± 222.26[a]	1478.23 ± 80.17[b]	1042.92 ± 132.12[c]
L1-L5 volume (mm^3)	3.27 ± 0.39	3.12 ± 0.11	2.69 ± 0.15
Motoneuron density	633.13 ± 104.46[a]	474.04 ± 19.78	391.13 ± 51.01

All the studied parameters (motoneuron number, volume of the L1-L5 ventral horn and motoneuron density) highlight that hMSC graft allows a delay of the motoneuron death compared with sal TG group. Data are reported as mean ± SEM; statistical analysis performed by means of one-way ANOVA and Newman-Keuls *post hoc* test. Motoneuron number: sal WT versus hMSC TG, [a]$P < 0.05$. hMSC TG versus sal TG, [b]$P < 0.05$. sal WT versus sal TG, [c]$P < 0.01$. Motoneuron density: sal WT versus sal TG, [a]$P < 0.05$.

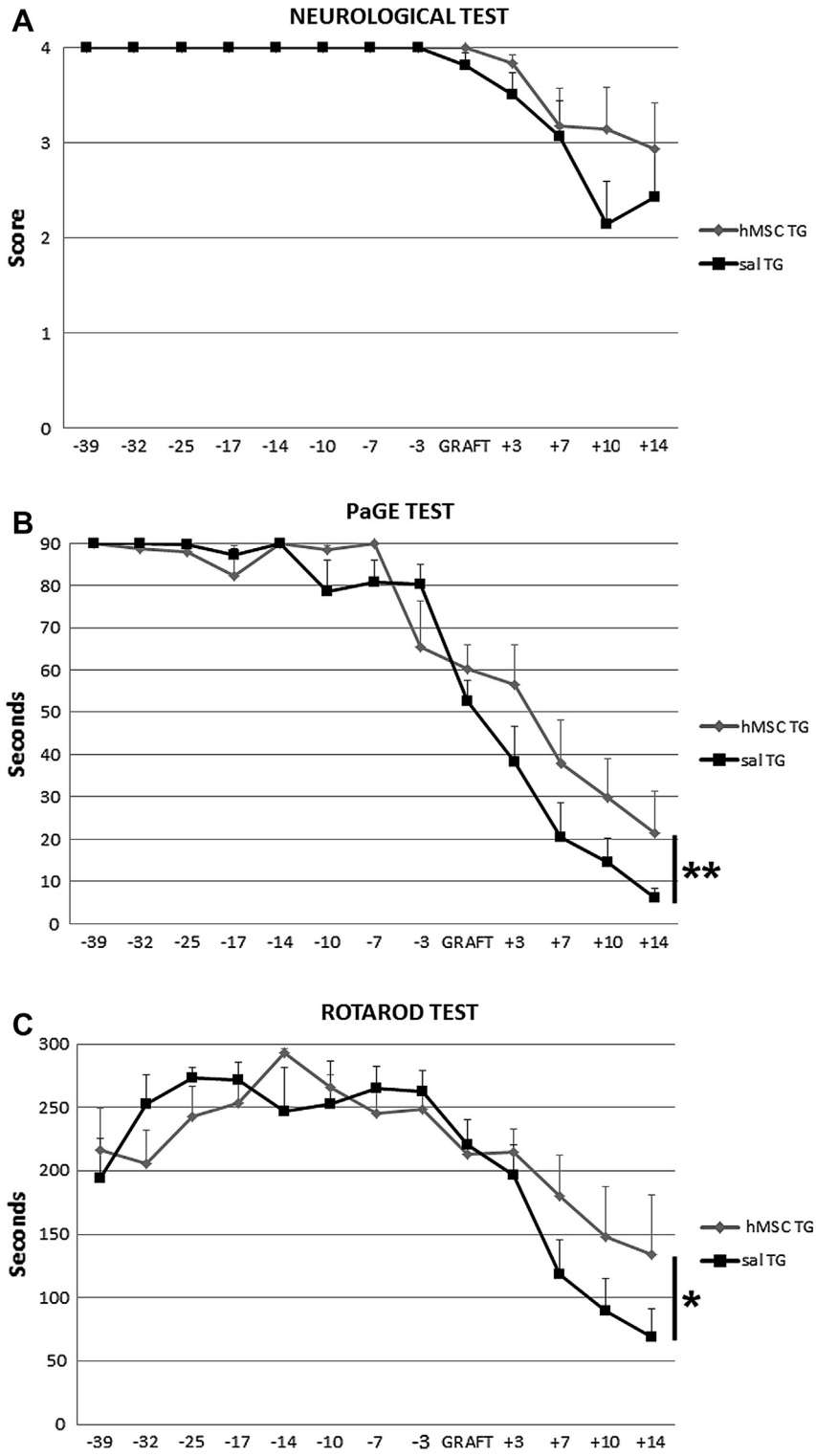

Figure 2. Behavioral tests. Functional recovery of hMSC TG (gray diamonds) and sal TG mice (black squares), studied with a battery of tests [neurological test (A), PaGE test (B) and rotarod test (C)]. The first values reported in the graph represent the scores obtained before symptom onset (from "−39 days" to "−3 days"), whereas the values reported at the "graft" time correspond to the last performance before graft. In every test after transplantation, treated mice show a delay in the motor impairment progression in comparison to sal TG group. Scores are expressed as mean ± SEM (*$P \leq 0.05$; **$P \leq 0.01$).

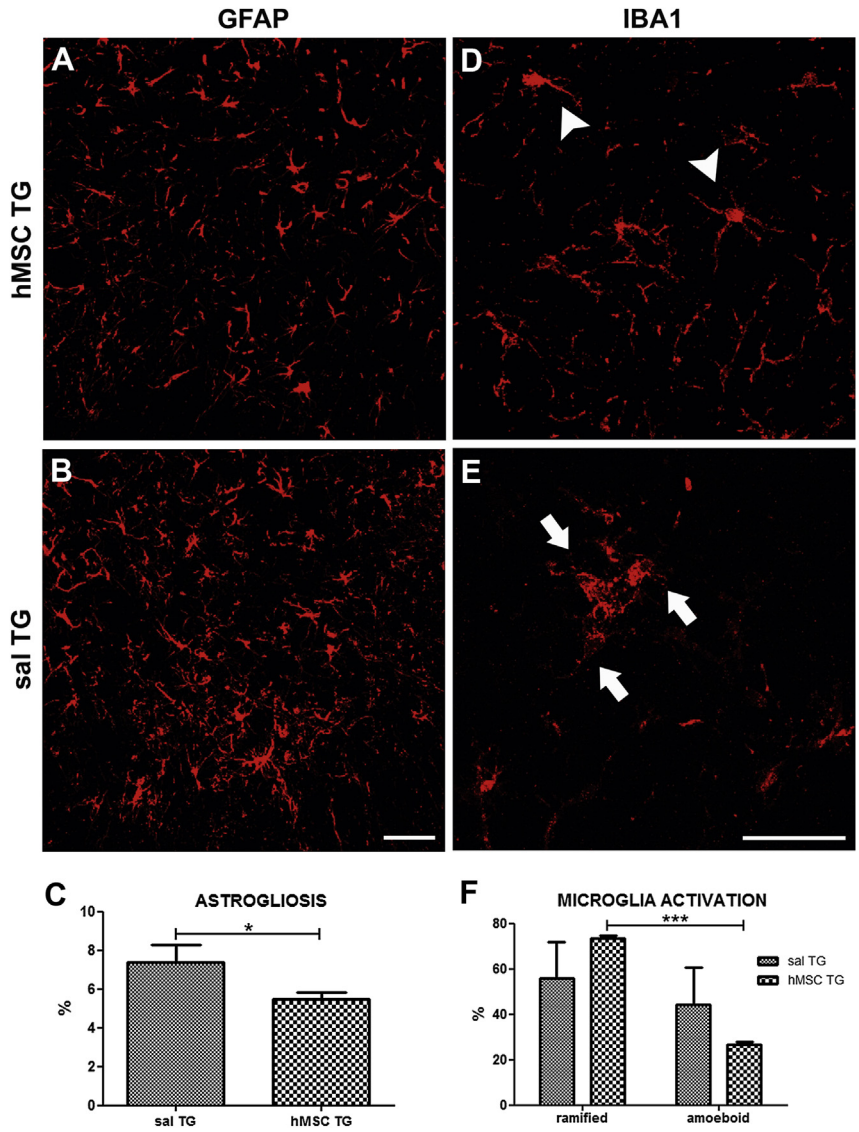

Figure 3. Astrogliosis and microglial activation analysis. Evaluation of reactive astrogliosis in terms of GFAP immunoreactivity and of microglia activation as measured by IBA1 immunoreactivity in the lumbar spinal cord of hMSC TG and sal TG mice. (A,B) The density of GFAP-immunopositive profiles is reduced in hMSC TG group (A) compared with the sal TG group (B). (C) Graph relative to astrogliosis. (D,E) The two groups show different patterns of microglial activation: hMSC TG mice are predominantly characterized by ramified microglia (arrowheads; D), whereas sal TG mice mostly display amoeboid microglia and, in some cases, in clusters (arrows; E). (F) Graph relative to microglia activation. Scale bar = 50 μm.

(Figure 3). The percentage of the overall GFAP-positive area was quantified with the use of Scion Image software for Windows by an observer blinded to the group identity of the specimens examined.

We quantified the densities of GFAP-immunopositive profiles at L5 level, in proximity to the injection site. The density was 7.39% ± 0.89% and 5.46% ± 0.38% in sal TG and hMSC TG mice, respectively (sal TG versus sal WT, $P < 0.05$) (Figure 3A,B).

Moreover, IBA1−positive microglial cells were classified as "ramified" and "amoeboid"; 73.4% ± 1.4% and 55.7% ± 16.2% ramified cells were found in hMSC TG and sal TG mice, respectively, and 26.6% ± 1.4% and 44.3% ± 16.2% amoeboid cells in hMSC TG and sal TG mice, respectively ("ramified" hMSC TG versus "amoeboid" hMSC TG, $P < 0.001$). In sal TG mice, we often observed abnormal clustering of hyperactivated amoeboid microglia (Figure 3D,E). The data are summarized in the graph in Figure 3C,F.

Cytokine expression in SOD mice transplanted with hMSCs

To characterize the mouse genes activated by hMSC transplantation in the cisterna lumbaris of SOD1 mice, we collected the RNA from the lumbar spinal

cord of sal WT, sal TG and hMSC TG mice. We pooled the cDNA of animals belonging to the same group for a first qualitative analysis with the use of a TaqMan Array Plate that allowed us to investigate the modulation of 92 mouse genes belonging to the immune response family. Actually, a large number of genes displayed very different expression levels in sal TG mice compared with sal WT mice; many immune-responsive genes were modulated by hMSC transplantation (data not shown), and we selected the genes that were strongly influenced by graft. The genes of the anti-inflammatory interleukins IL-10 and IL-13, the pro-inflammatory IL-12a and VEGF were further investigated by means of real-time PCR with the use of TaqMan specific assays. As shown in Figure 4A, IL-10 expression decreased 5-fold in sal TG compared with sal WT, whereas transplantation of hMSC restored IL-10 mRNA control levels (sal WT versus hMSC TG, $P < 0.05$). On the other hand, IL-12a expression was unchanged among the three experimental groups (Figure 4B), as first observed with the use of the array plate. On the contrary, IL-13 expression was slightly reduced in sal TG compared with sal WT and was strongly upregulated through hMSC transplantation (16- and 8-fold compared with sal TG and sal WT, respectively, $P < 0.05$; Figure 4C). Finally, VEGF mRNA levels were strongly (9-fold) downregulated in sal TG compared with sal WT (Figure 4C). hMSC TG mice showed upregulated VEGF levels (3-fold) compared with sal TG, even though they did not reach sal WT values ($P = 0.001$; Figure 4D).

Discussion

This study clearly confirms, with a less invasive experimental paradigm, the beneficial effects of hMSCs in the ALS model, previously demonstrated with intraparenchymal administration of the cells (6). Although others provided evidence for the molecular signature of hMSCs as a substrate for their paracrine role (33), we demonstrated that intracisternally delivered hMSCs modulate the expression of cytokines and, to a larger extent, of immunomodulatory molecules by the host, providing evidence for a putative mechanism of their action.

Experimental model

Even though genes other than those affecting mutations of SOD1 can give rise to familial ALS (34), animal models for these emerging forms are still lacking or do not reproduce the histopathological hallmarks of human disease. Therefore, for basic experimental studies, the SOD1 G93A mouse remains the most commonly used animal model (35). For this study, we used a slightly different model than in a previous one (6): the difference consists in the number of copies of mutated SOD1 (the previous model had approximately 30% fewer copies of the transgene construct than the present, as stated by Jackson Laboratory) and consequently in the time of onset of disease (14 weeks versus 28 weeks) and in the life expectancy (16 weeks versus 34 weeks). The time of administration of hMSCs was at the onset of

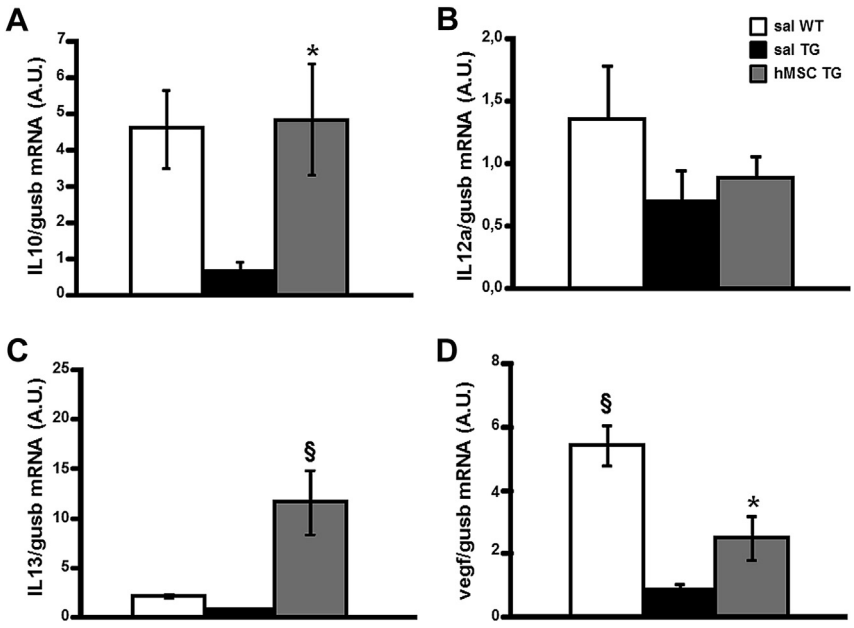

Figure 4. Expression analysis of IL-10, IL-12a, IL-13 and VEGF. mRNA expression levels of IL10, IL12a, IL13 and VEGF (A, B, C and D, respectively) in the lumbar spinal cord of WT and TG mice injected with saline (sal WT: white columns; sal TG: black columns) and in hMSC TG mice (gray columns). Each column represents mean ± SEM. *$P < 0.05$ hMSC TG versus sal TG; §$P < 0.05$ versus all groups.

symptoms. We expressly decided to treat the animals only at the inception of the disease because, at the moment, there is no way of anticipating the occurrence of disease in humans. The onset was detected, mouse by mouse, on the basis of behavioral tests, and not arbitrarily decided on the basis of the literature—such as at a predetermined age, because there is some inter-individual variability in the onset of disease (36) that might affect the study; the day in which the mouse showed at least two behavioral deficits in the hind limbs, for the second consecutive test session, was considered the day of disease onset (36).

hMSCs as drug delivery systems

To test a new method of administration, we injected hMSCs into the cisterna lumbaris. We previously reported the hMSC ability to survive and migrate after intraparenchymal transplantation into the lumbar spinal cord of presymptomatic SOD1 G93A mice, to prevent neuroinflammation, to delay the progressive decrease in the motoneuron number and to support a delay in motor impairment (6).

As reviewed by many authors, MSCs could represent a valid tool in view of a cell therapy approach in ALS, Parkinson disease, multiple sclerosis, spinal cord injury and stroke as the result of their immunomodulatory and neuroprotective potential. MSCs can release soluble molecules such as cytokines and chemokines and express immunorelevant receptors. Finally, they can release a number of neurotrophic and neuroprotective factors [nerve growth factor, brain-derived neurotrophic factor, glial cell line–derived neurotrophic factor, neurotrophin-3 and VEGF] that are essential for supporting motoneuron survival and delaying disease progression (37–39).

As previously shown (6), we did not provide immunosuppression to mice and we did not find any sign of immunoreaction to allogenic graft, even in the long term. hMSCs express low levels of human major histocompatibility complex class I and lack human major histocompatibility complex class II, do not express the CD40, CD80 or CD86 co-stimulatory molecules and are immunosuppressive. Nevertheless, there are some reports of immunorejection of hMSCs (40).

Comparison among different methods of administration

The local, intraparenchymal method of administration of stem cells aims directly at their target. We have shown that transplanted hMSCs, injected into the lumbar spinal cord (6) had beneficial effects on motoneuron survival, glial activation and motor behavior. The same approach was used in two open-label pilot studies in which hMSCs were injected with the use of a surgical procedure into different levels of the thoracic spinal cord of 19 patients with ALS (15,16). On the other hand, with this paradigm, we observed a limited craniocaudal diffusion, approximately 1 mm from the injection site, which might be relevant in mice (6) but requires multiple injection sites in patients (4,15), increasing the risk for side effects caused by surgery and penetration through the dorsal horn. Alternatively, genetically engineered hMSCs have been transplanted intramuscularly in a mouse model, leading to beneficial effects on muscle innervation, motoneuron survival and motor behavior (41).

Contrasting results have been obtained with intravenous delivery of MSCs. They are mostly trapped in the afferent vessels of the lungs and apparently are degraded there [our unpublished observations, 2012 (42)]. In the lungs, they can embolyze and cause endothelial damage (43). On the other hand, Uccelli *et al.* (5) showed that hMSCs injected intravenously in an ALS SOD1 mouse model improve motor function and survival of motoneurons, reduce ubiquitin aggregates and activate astrocytes and microglia. An immediate immunomodulatory effect induced by intravenous administration of MSCs has been shown in five patients with ALS by Karussis *et al.* (44).

Intrathecal delivery of high doses of hMSCs into the cisterna magna improves motoneuron survival, even though only few of them reach the spinal cord (45). hMSC transplantation into the cisterna magna of SOD1 rats through a catheter reaching the lumbar enlargement delayed motoneuron death and the decay in motor behavior and decreased microglial activation; moreover, hMSCs entered the spinal cord parenchyma and fused with astrocytes (46).

In the present study, we injected hMSCs in the cisterna lumbaris, and studied the effects on the histopathological parameters of the lumbar spinal cord. After 2 weeks from transplantation, we observed transplanted cells into the parenchyma, which suggests that not only diffusible factors can enter the spinal cord but also the hMSCs can migrate into the parenchyma to exert their paracrine activity. The finding of hMSCs through the whole lumbar spinal cord (and at a lesser extent at the lower thoracic level and rarely at the cervical level) suggests that the flux of the cerebrospinal fluid is bidirectional and allows, at least in mice, the transplanted cells to reach upper neuromers. Therefore, injection into the cisterna lumbaris allows more cell diffusion than the intraparenchymal procedure (6) and is the less invasive than the intraparenchymal and the intrathecal administrations and is more target-specific than intravenous delivery.

Anti-inflammatory, immunomodulatory and neuroprotective potential of hMSCs

ALS is a multi-factorial (47), non-cell autonomous disease, implicating that both microglial activation and astrogliosis are not mere epiphenomena of motoneuron death but play a pathogenetic role (48).

Therefore, it is relevant to provide evidence that hMSCs can play an immunomodulatory role in the disease, modulating both astrogliosis and microglial activation, as shown in the present study and in our previous report (6). To this aim, Uccelli *et al.* and others have characterized in detail the molecules that are secreted by hMSCs (see above). We further extend their findings, providing evidence that the host spinal cord modifies the expression of its neuroinflammatory and modulatory molecules as a consequence of hMSC transplantation. Even though specific cytokines can hardly be assigned to a pro- or anti-inflammatory role, in our experiments we observed consistent changes in their expression that suggest a beneficial role for their regulation by hMSCs.

Some authors have already demonstrated the MSC potential in exerting a paracrine influence on the microglial/astroglial function. For example, *in vitro* MSCs significantly increase microglial release of molecules associated with a neuroprotective phenotype such as CX3CR1, nuclear receptor 4 family, CD200 receptor and insulin growth factor 1. MSCs can modulate the microglial state, switching it from a detrimental phenotype to a neuroprotective one (49).

Indeed, microglia are resident brain cells that react to pathological tissue alterations. In physiological conditions, microglial cells display a "ramified resting" state; in most central nervous system disorders characterized by altered homeostasis, microglia become "activated," still ramified but with stouter cell processes; furthermore, fully activated microglia retract their cytoplasmic processes and become "amoeboid" (50). Microglial cells are Janus-faced cells that can exert both detrimental and beneficial effects: indeed, the literature describes cytotoxic classically activated M1 microglia and a neuroprotective alternatively activated M2 microglia (51). Such phenotypical bipartition is elicited by environmental signals, receptors expressed on microglial surface and the activated intracellular signaling pathways (52). In the case of classic activation, the transcription of inflammatory cytokines, such as tumor necrosis factor-α, IL-1β is induced, whereas in the case of alternative activation, the release of anti-inflammatory cytokines, such as IL-4, IL-10, and insulin-like growth factor 1, is promoted (51). Changes in cytokine expression such as IL-10 may be induced by hMSCs through the secretion of prostaglandin E2 (53).

This is in agreement with our findings. Indeed, we observed an increased level of endogenous IL-10, which could correlate with the different microglial morphology shown by hMSC TG and sal TG. hMSC TG microglia, characterized by a limited activation state, could provide a better neuroprotective effect compared with sal TG microglia, showing amoeboid and round morphologies. Similarly, Gomes-Leal (54) described different patterns of microglial activation after middle cerebral artery occlusion, associating the ramified/intermediate microglia to a downregulated inflammatory profile. The final phenotype would depend on both noxious and beneficial stimuli present in the extracellular space. Shaked *et al.* (55) suggest that moderate microglial activation allows for a better reaction in a hostile environment.

Recently, differences in the morphology of microglial cells, especially close to motoneurons, have been reported in pre-symptomatic SOD1 mice, thus suggesting an early involvement of microglia in the onset of disease (56). In agreement with our results, Dibaj *et al.* (57) found that after disease progression, microglial cells tend to switch to an ameboid phenotype and to cluster together.

On the other hand, Sun *et al.* (58), analyzing *in vitro* the MSC-conditioned medium influence on astrocytic gene expression, did not identify significant changes in IL-10 expression but, conversely, found a significant decrease in IL-6 expression. We also observed a slight downregulation of IL-6 after hMSC transplantation in TG mice (data not shown).

As concerns IL-13, in disagreement with our observations, in 2007, Shi *et al.* (59) reported an upregulation of IL-13 in peripheral blood CD4+ and CD8+ T cells in ALS, in correlation with the severity and progression of the disease. However, more recently, Fiala *et al.* (60) stimulated peripheral blood cells by mutant SOD1 and performed a microarray analysis of 28,869 genes: they observed a strong stimulation of expression of seven cytokines (IL-10, IL-23A, granulocyte-macrophage colony-stimulating factor, IL-1b, IL-1a, IL-6 and IL-7) but not of IL-13. Even though the neuroinflammatory role of IL-13 is still debated, in agreement with our results, there is evidence that MSCs, transplanted after spinal cord injury, can increase IL-13 levels and reduce tumor necrosis factor-α and IL-6 expression, in association with increased numbers of M2 macrophages (61).

Finally, there is evidence that VEGF expression represents a major therapeutic target in ALS. VEGF delivery in ALS experimental models can improve histopathological and behavioral phenotypes after intraventricular injection of VEGF-165–expressing adeno-associated virus serotype 4 vector (62), and

systemic administration of recombinant VEGF reduces astrogliosis and supports maintenance of neuromuscular junctions (63,64). Our present results suggest that hMSCs can induce an upregulation in the expression of VEGF by the host, which might protect motoneurons and delay their cell death.

Conclusions

On the basis of the present study, by intracisternal delivery, hMSCs can provide beneficial therapeutic effects. Moreover, our results support the idea that MSCs, besides playing a bystander role and delivering neuroprotective and immunomodulatory molecules to the host, elicit a response by the host, modifying its cellular and molecular response to disease. Further studies are needed to fully identify the cell-derived bioactive factors to be used as drugs. The identification of the key molecules delivered by MSCs could allow designing pharmaceutical protocols that mimic the MSC mode of action (65). On the other hand, as a distinct advantage over pharmacological therapy, MSCs can be modulated by the environment and tune their paracrine role to the needs of the host.

Acknowledgments

This work was partially supported by Rete Oncologica del Piemonte e della Valle d'Aosta network and Compagnia di San Paolo Foundation (Turin) grants to FF and by an Italian Ministry of University and Research (MIUR) grant to A. Vercelli.

Disclosure of interests: The authors have no commercial, proprietary, or financial interest in the products or companies described in this article.

References

1. Rowland LP, Shneider NA. Amyotrophic lateral sclerosis. N Engl J Med. 2001;344:1688–700.
2. Bensimon G, Lacomblez L, Meininger V. ALS/Riluzole Study Group. A controlled trial of riluzole in amyotrophic lateral sclerosis. N Engl J Med. 1994;330:585–91.
3. Kim SU, de Vellis J. Stem cell-based cell therapy in neurological diseases: a review. J Neurosci Res. 2009;87:2183–200.
4. Mazzini L, Vercelli A, Ferrero I, Boido M, Cantello R, Fagioli F. Transplantation of mesenchymal stem cells in ALS. In: Dunnett S, Björklund A, editors. Functional neural transplantation III: primary and stem cell transplantation for brain repair. Progr Brain Res. 2012;201:333–359.
5. Uccelli A, Milanese M, Principato MC, Morando S, Bonifacino T, Vergani L, et al. Intravenous mesenchymal stem cells improve survival and motor function in experimental amyotrophic lateral sclerosis. Mol Med. 2012;18:794–804.
6. Vercelli A, Mereuta OM, Garbossa D, Muraca G, Mareschi K, Rustichelli D, et al. Human mesenchymal stem cell transplantation extends survival, improves motor performance and decreases neuroinflammation in mouse model of amyotrophic lateral sclerosis. Neurobiol Dis. 2008;31:395–405.
7. Zhao CP, Zhang C, Zhou SN, Xie YM, Wang YH, Huang H, et al. Human mesenchymal stromal cells ameliorate the phenotype of SOD1-G93A ALS mice. Cytotherapy. 2007;9:414–26.
8. Hefferan MP, Galik J, Kakinohana O, Sekerkova G, Santucci C, Marsala S, et al. Human neural stem cell replacement therapy for amyotrophic lateral sclerosis by spinal transplantation. PLoS One. 2012;7:e42614.
9. Hwang DH, Lee HJ, Park IH, Seok JI, Kim BG, Joo IS, et al. Intrathecal transplantation of human neural stem cells overexpressing VEGF provide behavioral improvement, disease onset delay and survival extension in transgenic ALS mice. Gene Ther. 2009;16:1234–44.
10. Mitrecić D, Nicaise C, Gajović S, Pochet R. Distribution, differentiation, and survival of intravenously administered neural stem cells in a rat model of amyotrophic lateral sclerosis. Cell Transplant. 2010;19:537–48.
11. Teng YD, Benn SC, Kalkanis SN, Shefner JM, Onario RC, Cheng B, Lachyankar MB, Marconi M, Li J, Yu D, Han I, Maragakis NJ, Lládo J, Erkmen K, Redmond DE Jr, Sidman RL, Przedborski S, Rothstein JD, Brown RH Jr, Snyder EY. Multimodal actions of neural stem cells in a mouse model of ALS: a meta-analysis. Sci Transl Med. 2012 Dec 19;4(165):165ra164.
12. Li Y, Bao J, Khatibi NH, Chen L, Wang H, Duan Y, et al. Olfactory ensheathing cell transplantation into spinal cord prolongs the survival of mutant SOD1(G93A) ALS rats through neuroprotection and remyelination. Anat Rec. 2011;294:847–57.
13. Papadeas ST, Maragakis NJ. Advances in stem cell research for amyotrophic lateral sclerosis. Curr Opin Biotechnol. 2009;20:545–51.
14. Feng Z, Gao F. Stem cell challenges in the treatment of neurodegenerative disease. CNS Neurosci Ther. 2012;18:142–8.
15. Mazzini L, Ferrero I, Luparello V, Rustichelli D, Gunetti M, Mareschi K, et al. Mesenchymal stem cell transplantation in amyotrophic lateral sclerosis: a phase I clinical trial. Exp Neurol. 2010;223:229–37.
16. Mazzini L, Mareschi K, Ferrero I, Miglioretti M, Stecco A, Servo S, et al. Mesenchymal stromal cell transplantation in amyotrophic lateral sclerosis: a long-term safety study. Cytotherapy. 2012;14:56–60.
17. Pittenger MF, Mackay AM, Beck SC, Jaiswal RK, Douglas R, Mosca JD, et al. Multilineage potential of adult human mesenchymal stem cells. Science. 1999;284:143–7.
18. Otto WR, Wright NA. Mesenchymal stem cells: from experiment to clinic. Fibrogenesis Tissue Repair. 2011;4:20.
19. Weydt P, Hongso Y, Kliot M, Moller T. Assessing disease onset and progression in the SOD1 mouse model of ALS. Neuroreport. 2003;14:1051–4.
20. Busletta C, Novo E, Valfrè Di Bonzo L, Povero D, Paternostro C, Ievolella M, et al. Dissection of the biphasic nature of hypoxia-induced motogenic action in bone marrow-derived human mesenchymal stem cells. Stem Cells. 2011;29:952–63.
21. Ferrero I, Mazzini L, Rustichelli D, Gunetti M, Mareschi K, Testa L, et al. Bone marrow mesenchymal stem cells from healthy donors and sporadic amyotrophic lateral sclerosis patients. Cell Transplant. 2008;17:255–66.
22. Mareschi K, Rustichelli D, Calabrese R, Gunetti M, Sanavio F, Errichiello E, et al. Mesenchymal stem cell

expansion by plating whole bone marrow at a low cellular density: a more advantageous method for clinical use. Stem Cells Int. 2012;2012:920581.
23. Morita E, Watanabe Y, Ishimoto M, Nakano T, Kitayama M, Yasui K, et al. A novel cell transplantation protocol and its application to an ALS mouse model. Exp Neurol. 2008;213: 431–8.
24. Habisch HJ, Janowski M, Binder D, Kuzma-Kozakiewicz M, Widmann A, Habich A, et al. Intrathecal application of neuroectodermally converted stem cells into a mouse model of ALS: limited intraparenchymal migration and survival narrows therapeutic effects. J Neural Transm. 2007;114:1395–406.
25. Lee IO, Lim ES. Intracisternal or intrathecal glycine, taurine, or muscimol inhibit bicuculline-induced allodynia and thermal hyperalgesia in mice. Acta Pharmacol Sin. 2010;31: 907–14.
26. Ciavarro GL, Calvaresi N, Botturi A, Bendotti C, Andreoni G, Pedotti A. The densitometric physical fractionator for counting neuronal populations: application to a mouse model of familial amyotrophic lateral sclerosis. J Neurosci Meth. 2003;129:61–71.
27. West MJ, Slomianka L, Gundersen HJ. Unbiased stereological estimation of the total number of neurons in the subdivisions of the rat hippocampus using the optical fractionator. Anat Rec. 1991;231:482–97.
28. Dominici M, Le Blanc K, Mueller I, Slaper-Cortenbach I, Marini F, Krause D, et al. Minimal criteria for defining multipotent mesenchymal stromal cells: the International Society for Cellular Therapy position statement. Cytotherapy. 2006;8:315–7.
29. Castanheira P, Torquetti LT, Magalhães DR, Nehemy MB, Goes AM. DAPI diffusion after intravitreal injection of mesenchymal stem cells in the injured retina of rats. Cell Transplant. 2009;18:423–31.
30. Jiang Y, Lv H, Huang S, Tan H, Zhang Y, Li H. Bone marrow mesenchymal stem cells can improve the motor function of a Huntington's disease rat model. Neurol Res. 2011;33:331–7.
31. Leiker M, Suzuki G, Iyer VS, Canty JM Jr, Lee T. Assessment of a nuclear affinity labeling method for tracking implanted mesenchymal stem cells. Cell Transplant. 2008;17:911–22.
32. Qin ZH, Qu JM, Xu JF, Zhang J, Summah H, Sai-Yin HX, et al. Intrapleural delivery of mesenchymal stem cells: a novel potential treatment for pleural diseases. Acta Pharmacol Sin. 2011;32:581–90.
33. Pedemonte E, Benvenuto F, Casazza S, Mancardi G, Oksenberg JR, Uccelli A, et al. The molecular signature of therapeutic mesenchymal stem cells exposes the architecture of the hematopoietic stem cell niche synapse. BMC Genomics. 2007;8:65.
34. Chiò A, Calvo A, Mazzini L, Cantello R, Mora G, Moglia C, et al. Extensive genetics of ALS: a population-based study in Italy. Neurology. 2012;79:1983–9.
35. Boido M, Buschini E, Piras A, Spigolon G, Valsecchi V, Mazzini L, et al. Advantages and pitfalls in experimental models of ALS. In: Maurer MH, editor. Amyotrophic Lateral Sclerosis. InTech; 2012. p. 125–56.
36. Valsecchi V, Boido M, Piras A, Spigolon G, Vercelli A. Motor and molecular analysis to detect the early symptoms in a mouse amyotrophic lateral sclerosis model. Health. 2013;5: 10A3.
37. Garbossa D, Boido M, Fontanella M, Fronda C, Ducati A, Vercelli A. Recent therapeutic strategies for spinal cord injury treatment: possible role of stem cells. Neurosurg Rev. 2012; 35:293–311.
38. Joyce N, Annett G, Wirthlin L, Olson S, Bauer G, Nolta JA. Mesenchymal stem cells for the treatment of neurodegenerative disease. Regen Med. 2010;5:933–46.
39. Mazzini L, Vercelli A, Ferrero I, Mareschi K, Boido M, Servo S, et al. Stem cells in amyotrophic lateral sclerosis: state of the art. Expert Opin Biol Ther. 2009;9:1245–58.
40. Uccelli A, Pistoia V, Moretta L. Mesenchymal stem cells: a new strategy for immunosuppression? Trends Immunol. 2007;28:219–26.
41. Suzuki M, McHugh J, Tork C, Shelley B, Klein SM, Aebischer P, et al. GDNF secreting human neural progenitor cells protect dying motor neurons, but not their projection to muscle, in a rat model of familial ALS. PLoS One. 2007;2: e689.
42. Lee RH, Pulin AA, Seo MJ, Kota DJ, Ylostalo J, Larson BL, et al. Intravenous hMSCs improve myocardial infarction in mice because cells embolized in lung are activated to secrete the anti-inflammatory protein TSG-6. Cell Stem Cell. 2009;5: 54–63.
43. Schrepfer S, Deuse T, Reichenspurner H, Fischbein MP, Robbins RC, Pelletier MP. Stem cell transplantation: the lung barrier. Transplant Proc. 2007;39:573–6.
44. Karussis D, Karageorgiou C, Vaknin-Dembinsky A, Gowda-Kurkalli B, Gomori JM, Kassis I, et al. Safety and immunological effects of mesenchymal stem cell transplantation in patients with multiple sclerosis and amyotrophic lateral sclerosis. Arch Neurol. 2010;67:1187–94.
45. Kim H, Kim HY, Choi MR, Hwang S, Nam KH, Kim HC, et al. Dose-dependent efficacy of ALS-human mesenchymal stem cells transplantation into cisterna magna in SOD1-G93A ALS mice. Neurosci Lett. 2010;468:190–4.
46. Boucherie C, Schäfer S, Lavand'homme P, Maloteaux JM, Hermans E. Chimerization of astroglial population in the lumbar spinal cord after mesenchymal stem cell transplantation prolongs survival in a rat model of amyotrophic lateral sclerosis. J Neurosci Res. 2009;87:2034–46.
47. Eisen A. Amyotrophic lateral sclerosis is a multifactorial disease. Muscle Nerve. 1995;18:741–52.
48. Ilieva H, Polymenidou M, Cleveland DW. Non-cell autonomous toxicity in neurodegenerative disorders: ALS and beyond. J Cell Biol. 2009;187:761–72.
49. Giunti D, Parodi B, Usai C, Vergani L, Casazza S, Bruzzone S, et al. Mesenchymal stem cells shape microglia effector functions through the release of CX3CL1. Stem Cells. 2012;30:2044–53.
50. Ransohoff RM, Perry VH. Microglial physiology: unique stimuli, specialized responses. Annu Rev Immunol. 2009;27: 119–45.
51. Henkel JS, Beers DR, Zhao W, Appel SH. Microglia in ALS: the good, the bad, and the resting. J Neuroimmune Pharmacol. 2009;4:389–98.
52. David S, Kroner A. Repertoire of microglial and macrophage responses after spinal cord injury. Nat Rev Neurosci. 2011;12: 388–99.
53. Uccelli A, Moretta L, Pistoia V. Mesenchymal stem cells in health and disease. Nat Rev Immunol. 2008;8:726–36.
54. Gomes-Leal W. Microglial physiopathology: how to explain the dual role of microglia after acute neural disorders? Brain Behav. 2012;2:345–56.
55. Shaked I, Porat Z, Gersner R, Kipnis J, Schwartz M. Early activation of microglia as antigen-presenting cells correlates with T cell-mediated protection and repair of the injured central nervous system. J Neuroimmunol. 2004;146:84–93.
56. Gerber YN, Sabourin JC, Rabano M, Vivanco MD, Perrin FE. Early functional deficit and microglial disturbances in a mouse model of amyotrophic lateral sclerosis. PLoS One. 2012;7:e36000.
57. Dibaj P, Steffens H, Zschüntzsch J, Nadrigny F, Schomburg ED, Kirchhoff F, et al. In vivo imaging reveals distinct inflammatory activity of CNS microglia versus PNS

macrophages in a mouse model for ALS. PLoS One. 2011;6:e17910.
58. Sun H, Bénardais K, Stanslowsky N, Thau-Habermann N, Hensel N, Huang D, et al. Therapeutic potential of mesenchymal stromal cells and MSC conditioned medium in amyotrophic lateral sclerosis (ALS): in vitro evidence from primary motor neuron cultures, NSC-34 cells, astrocytes and microglia. PLoS One. 2013;8:e72926.
59. Shi N, Kawano Y, Tateishi T, Kikuchi H, Osoegawa M, Ohyagi Y, et al. Increased IL-13-producing T cells in ALS: positive correlations with disease severity and progression rate. J Neuroimmunol. 2007;182:232–5.
60. Fiala M, Chattopadhay M, La Cava A, Tse E, Liu G, Lourenco E, et al. IL-17A is increased in the serum and in spinal cord CD8 and mast cells of ALS patients. J Neuroinflammation. 2010;7:76.
61. Nakajima H, Uchida K, Guerrero AR, Watanabe S, Sugita D, Takeura N, et al. Transplantation of mesenchymal stem cells promotes an alternative pathway of macrophage activation and functional recovery after spinal cord injury. J Neurotrauma. 2012;29:1614–25.
62. Dodge JC, Treleaven CM, Fidler JA, Hester M, Haidet A, Handy C. AAV4-mediated expression of IGF-1 and VEGF within cellular components of the ventricular system improves survival outcome in familial ALS mice. Mol Ther. 2010;18:2075–84.
63. Xie Y, Weydt P, Howland DS, Kliot M, Möller T. Inflammatory mediators and growth factors in the spinal cord of G93A SOD1 rats. NeuroReport. 2004;15:2513–6.
64. Zheng C, Sköld MK, Li J, Nennesmo I, Fadeel B, Henter JI. VEGF reduces astrogliosis and preserves neuromuscular junctions in ALS transgenic. Biochem Biophys Res Commun. 2007;363:989–93.
65. Bianco P, Cao X, Frenette PS, Mao JJ, Robey PG, Simmons PJ, et al. The meaning, the sense and the significance: translating the science of mesenchymal stem cells into medicine. Nat Med. 2013;19:35–42.